Acoustical propagation in a prefractal waveguide

Vincent Gibiat*
Laboratoire Ondes et Acoustique, ESPCI, Université Paris 7, UMR CNRS 7587, 10, Rue Vauquelin, 75231 Paris Cedex 05, France

Ana Barjau†
Laboratorio de Mecánica y Vibroacústica, Universidad Politécnica de Catalunya, Diagonal, 647, 08028 Barcelona, Spain

Kaelig Castor and Etienne Bertaud du Chazaud
Laboratoire Ondes et Acoustique, ESPCI, Université Paris 7, UMR CNRS 7587, 10, Rue Vauquelin, 75231 Paris Cedex 05, France
(Received 7 May 2002; revised manuscript received 10 March 2003; published 27 June 2003)

We present a theoretical study and experimental results for an acoustic multiscattering one-dimensional system made of cylindrical tubes of different diameters whose lengths follow a Cantor-like structure. Homothetic acoustical features and forbidden bands as well as wave trapping phenomena are reported.

DOI: 10.1103/PhysRevE.67.066609 PACS number(s): 42.65.Wi

I. INTRODUCTION

Recently, a large number of publications has extensively studied the vibrational properties of fractal objects [1–3]. In addition to this work, which shows the importance of and the interest of the scientific community in such systems, more recent papers have pointed out the peculiar characteristics of acoustical propagation in fractals [4,5]. Such concepts as fractons, fractinos, or occurrences of known phenomena such as ''wave localization'' have been defined, reported, and studied.

From the later work, one can distinguish two different types of fractal object: those limited by boundaries with fractal geometry (boundary fractals), such as those mainly studied by Sapoval *et al.* [6], and those with dynamical properties varying according to a fractal rule (mass fractals). In acoustics, mass fractals have been studied only by Alippi *et al.* [2,4]. In boundary fractals, wave propagation is described by a classical second order differential equation, while in the second case, the fractality of the medium in principle does not allow a differential formulation. Nevertheless, it is always possible to write the mathematical problem associated with the acoustical one from a probabilistic point of view, or to study the problem through perturbation techniques.

Among fractal structures, the simplest one [which can be embedded in a one-dimensional (1D) space] is the Cantor set. A Cantor-like system is a system that has been built through the same kind of hierarchical rules but with a finite number of iterations. Even if it has not reached the real fractal state, it shows interesting acoustical propagation properties, as shown by Alippi *et al.* [2].

In Alippi *et al.*'s work, the Cantor-like structure was applied to a 3D mechanical system made up of alternating expoxy and piezoceramic layers for ultrasonic purposes. Even if the geometry follows the scheme of the Cantor set, volume and surface waves may be simultaneously produced, which may make difficult the interpretation of the results and their comparison with numerical simulations.

In any case, it is interesting to verify if the behaviors observed in these works are also found in the case of low frequency propagation through air. We have chosen to study aerial propagation using a waveguide made of cylindrical tubes of different diameters as the acoustical structure.

The main aim of this paper is to study the transport properties of an acoustical wave through a one-dimensional waveguide with self-similarity properties. In particular, we will verify that the self-similar structure of the waveguide shows up in the frequency responses and that wave trapping is possible in such structures.

We studied the problem from both a theoretical and an experimental point of view. Numerical simulations were done and compared to the experimental results in order to validate the numerical model and to then derive results that cannot be obtained without perturbing the experimental system.

II. THE ACOUSTICAL CANTOR-LIKE WAVEGUIDE

A quasi-Cantor system where 1D propagation is possible can be obtained through cylindrical air tubes whenever the wavelength is such that the first transverse mode is not excited. This implies a frequency lower than $f=\gamma_{1,0}c/2\pi r$ where $\gamma_{1,0}$ is the first zero of the first derivative of the Bessel function J_0, c is the speed of sound, and r is the radius of the cylinder (in our case this leads to a cutoff frequency of around 6 kHz for the largest diameter of our waveguide). Such an acoustical waveguide behaves purely as a 1D system, that is, only the plane mode (1,0,0) is a propagating one when the above condition is satisfied.

The iterative process to build a Cantor system is the following. From a uniform tube (whose length L will be taken as the unit length measure), the central third is removed and replaced by a larger tube (Cantor order 1). Then the operation is repeated with the two remaining narrow spans, thus generating a Cantor order 2, and so on (Fig. 1). In this case,

*Present address: LAMI, Université Paul Sabatier, 118 route de Narbonne, 31062 Toulouse Cedex, France. Electronic address: Vincent.Gibiat@espci.fr
†Electronic address: ana.barjau@upc.es

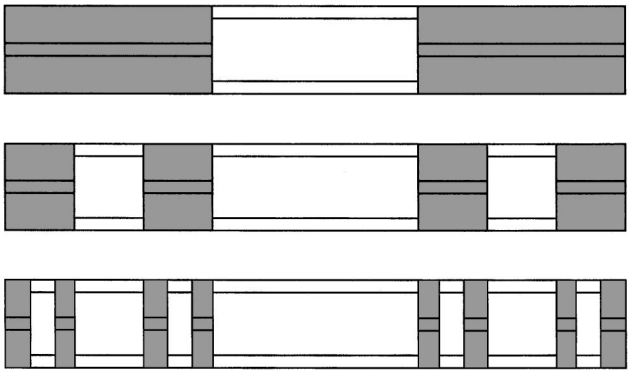

FIG. 1. Several steps of the building process of the Cantor acoustical waveguide.

changes in the physical characteristics of the medium are obtained through changes in the tube diameter and thus impedance mismatch between the two sides of the diameter discontinuities.

It is obvious that this building process cannot be iterated up to infinity (the real fractal state). Actually, it is not necessary for the purpose of our experimental study, since after a few iterations, the shortest parts of the system become much smaller than the wavelengths concerned and so are not relevant for the propagation problem.

The study of this quasi-Cantor waveguide has to be done through experimental measurements of various frequency responses (the acoustical input impedance and the reflection and transmission coefficients) and their equivalent time-domain responses. As noninvasive acoustical measurements can be done only at the ends of the waveguide, the acoustical pressure distribution inside the system can be obtained only through numerical simulation.

These two approaches are necessary and complementary. Typically, one measures in the frequency domain the input acoustical impedance $\tilde{Z}(\omega)=\tilde{p}(\omega)/\tilde{v}(\omega)$, where $\tilde{p}(\omega)$ and $\tilde{v}(\omega)$ are the acoustical pressure and velocity and ω is the pulsation, with different end conditions (anechoic end, open end, closed end). One can then derive the global reflection coefficient of the structure (frequency domain), $\tilde{R}(\omega)$, or its global reflection function (time domain), $R(t)$. Such measurements are unavoidable in order to properly assess the validity of the numerical model. Once they have been done, a confident exploration of the internal wave propagation is possible.

We worked with an initial cylinder of 999 mm length and 10 mm diameter. The larger tubes have a 28 mm diameter. This leads to a section ratio $\sigma=S/s\approx 9$ and specific impedance ratio $Z_S/Z_s=s/S\approx 1/9$. Quasi-Cantor structures have been built up to order 5 and measured in the [20 Hz, 2500 Hz] frequency range, which is sufficiently low to ensure 1D propagation.

Such a simple system allows a very basic numerical simulation. It can be seen as a real unit segment with punctual localized scatterers placed at each impedance mismatch (or diameter discontinuity). An impulsional acoustical pressure wave which interacts with a scatterer generates a two-part scattered wave: one that propagates in the same direction as the incident one (transmitted wave) and another one propagating in the opposite direction (reflected wave). The incident wave and the reflected wave have opposite signs when the scatterer corresponds to a section widening. When it corresponds to a narrowing, they share the same sign.

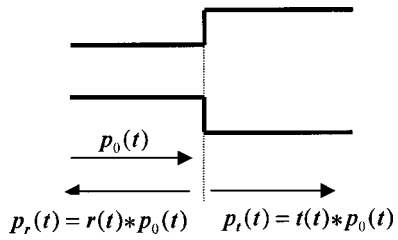

FIG. 2. Reflection-transmission process at a diameter discontinuity.

From an acoustical point of view the problem is then seen as a reflection-transmission process at an interface. The local reflection and transmission functions associated with each scatterer [$r(t)$ and $t(t)$, respectively] can be easily obtained from the traditional constant-pressure and continuity-flow equations at the interface—the Kirchhoff conditions (Fig. 2)—$r(t)=[(s-S)/(s+S)]\delta(t)$ and $t(t)=[2S/(s+S)]\delta(t)$ where s and S are the small and wide sections, respectively. Although $t(t)$ is always positive, $r(t)$ can have either a positive or a negative sign in our 1D Cantor-like tube.

The following results thus correspond to a double problem: on one hand a very general abstract problem (that of 1D multiscattering) of wide importance in physics and on the other hand an experimentally acoustical feasible problem. Thus one can expect that our results should be easy to shift to other fields of physics.

III. THEORETICAL AND EXPERIMENTAL STUDY OF ACOUSTICAL PROPAGATION THROUGH A CANTOR-LIKE WAVEGUIDE

A. General considerations

The classical wave equation is the starting point to study acoustical propagation in waveguides. It can be reduced to its 1D formulation whenever the conditions mentioned before (Sec. II) are satisfied and the geometry is not too far from cylindrical. When the departures from the uniform cylindrical profile are small enough to be considered as perturbations, it is possible to describe the problem with one single differential equation and solve it, for example, through a perturbation method [7]. For the case of the Cantor waveguide, this would call for a small value of $(S-s)/S$. In our case this approach is not applicable as the two particular section values s and S lead to $(S-s)/S=0.9$.

Another traditional way to deal with this problem is to consider separately the exact general solution for each elementary cylindrical span and couple them at the discontinuities through the Kirchhoff conditions. In the frequency domain, this method is generally formulated through transfer matrices, whereas in the time domain, it is usually written in terms of reflection and transmission functions (as mentioned

at the end of the previous section). It is obvious that both techniques are equivalent and simply related through a Fourier transform.

B. Frequency-domain results

The transfer matrix of a 1D acoustical system relates the acoustical variables, pressure and velocity, at the input and output sections:

$$\begin{pmatrix} \tilde{p}(\omega) \\ \tilde{v}(\omega) \end{pmatrix}_{input} = \begin{pmatrix} T_{11}(\omega L) & T_{12}(\omega L) \\ T_{21}(\omega L) & T_{22}(\omega L) \end{pmatrix} \begin{pmatrix} \tilde{p}(\omega) \\ \tilde{v}(\omega) \end{pmatrix}_{output} \equiv (T(\omega L)) \begin{pmatrix} \tilde{p}(\omega) \\ \tilde{v}(\omega) \end{pmatrix}_{output},$$

where L is the total length of the system. This matrix is obtained through the product of two types of elementary matrices: those corresponding to the cylindrical parts and those representing the Kirchhoff conditions at the diameter discontinuities (see, for example, [8]) The 1D system is fully characterized through this matrix with arbitrary end conditions. The eigenfrequencies are obtained from an equation on $T_{i,j}$, usually transcendental in ω, by imposing particular end conditions. This equation in general needs a numerical resolution. However, the eigenmodes (the pressure and velocity distributions along the waveguide) call for a point to point study of the elementary matrices.

The lack of periodicity makes difficult a general study of the transfer matrix structure. However, if losses are neglected, a few general considerations can be made for the case of our Cantor waveguides.

If $(T_n(\omega L))$ is the transfer matrix of a Cantor waveguide of order n, then that corresponding to the following order $(n+1)$ is obtained as

$$(T_{n+1}(\omega L)) = (T_n(\omega L/3))(D(S/s))(C(\omega L/3)) \times (D(s/S))(T_n(\omega L/3))$$

with

$$(C(\omega L)) = \begin{pmatrix} \cos(\omega L/c) & iZ_0 \sin(\omega L/c) \\ (i/Z_0)\sin(\omega L/c) & \cos(\omega L/c) \end{pmatrix}$$

and

$$(D(S_a/S_b)) = \begin{pmatrix} 1 & 0 \\ 0 & S_a/S_b \end{pmatrix},$$

where $Z_0 = \rho c$ is the characteristic impedance of the transmission medium, here air. The factor (1/3), appearing in the (T_n) argument, denotes the homothetical reduction of the waveguide order n in order to obtain the following iteration, and that appearing in the central matrix expresses just the fact that the central cylindrical span has a constant length equal to one-third of the global length L.

For a Cantor order 1, $(T_1(\omega L))$ is

$$(T_1(\omega L)) = (C(\omega L/3))(D(S/s))(C(\omega L/3)) \times (D(s/S))(C(\omega L/3)).$$

It is easy to verify that this matrix has a structure of the form $(T_1(\omega L)) = \left(\begin{smallmatrix} f_1 & ig_1 \\ ih_1 & f_1 \end{smallmatrix}\right)$, where f_1, g_1, h_1 are real functions of (ωL). This structure is not modified by the homotethy. As the product of the three central matrices $(D)(C)(D)$ shows the same features, the transfer matrix for the nth order will also be of the form $(T_n(\omega L)) = \left(\begin{smallmatrix} f_n & ig_n \\ ih_n & f_n \end{smallmatrix}\right)$. Moreover, the symmetry of our waveguides implies that $(T_n(\omega L))^{-1} = (T_n(-\omega L))$, and consequently $\det(T_n(\omega L)) = f_n^2 + g_n h_n = 1$.

Nothing general can be said in principle about the eigenproblem. The calculation of the eigenfrequencies for each order has to be done from the precise form of the transfer matrix elements. However, the exploration of the first three orders allows an interesting extrapolation to higher ones.

Let us assume that both ends of the waveguide are open. This condition can be roughly formulated as a zero pressure at the input and output sections, and the equation giving the eigenfrequencies is $T_{12}(\omega) = 0$. For Cantor order 1, the resulting transcendental equation is

$$T_{12}(\omega) = iZ_0 \frac{S}{s}\left[\left(1+\frac{s}{S}\right)^2 \cos^2\left(\frac{\omega L}{3c}\right) - 1\right]\sin\left(\frac{\omega L}{3c}\right) = 0.$$

This defines two families of frequencies, one satisfying the condition $\sin(\omega L/3c) = 0$ and another satisfying $(1+s/S)^2 \cos^2(\omega L/3c) = 1$. The solutions for the first condition are $\tilde{\omega}_m = (3c/L)m\pi$, and those for the second one are

$$\omega_m^+ = \frac{3c}{L}\left[m\pi + \cos^{-1}\left(\frac{S}{S+s}\right)\right],$$

$$\omega_m^- = \frac{3c}{L}\left[m\pi - \cos^{-1}\left(\frac{S}{S+s}\right)\right],$$

with the m integer varying from 0 to infinity in all cases.

The family corresponding to $\tilde{\omega}_m$ contains the same resonance frequencies that would have any of the three elementary spans if isolated with open or closed ends. The other family, containing ω_m^+ and ω_m^-, corresponds to pairs of frequencies close to those of the first family but shifted upward and downward, respectively, as a consequence of the coupling factor $S/(S+s)$.

The same calculations for orders $n=2$ and $n=3$ show that the element $T_{12}(\omega)$ is always of the form $T_{12}(\omega) = F(\omega)\sin(\omega L/3^n c)$, and so the first family of frequencies $\tilde{\omega}_m = (3^n c/L)m\pi$ will always be part of the waveguide eigenfrequencies. In this case, these frequencies correspond to the resonance frequencies that would have the shortest cylindrical spans of the system (that is, with length equal to $L/3^n$) if isolated and with open or closed ends. As

the other spans have lengths that are integer multiples of $L/3^n$, this family of frequencies also coincides with the higher harmonics of the longer parts (if isolated and with open or closed ends, of course).

This result can be extrapolated to higher orders. However, there is no simple general form for the equation defining the second family.

For Cantor order 1 with closed ends, the eigenfrequencies are defined by

$$T_{21}(\omega)=i\frac{1}{Z_0}\frac{s}{S}\left[\left(1+\frac{S}{s}\right)^2\cos^2\left(\frac{\omega L}{3c}\right)-1\right]\sin\left(\frac{\omega L}{3c}\right)=0.$$

Again we have two families of frequencies, and the same kinds of comments that have been made for the open end case can be made now.

The same calculations for orders $n=2$ and $n=3$ with closed ends show that the first family of frequencies $\tilde{\omega}_m=(3^n c/L)m\pi$ will always be part of the waveguide eigenfrequencies.

Finally, for the case of anechoic ends, the eigenfrequency equation is $Z_0=[Z_0T_{11}(\omega)+T_{12}(\omega)]/[Z_0T_{21}(\omega)+T_{22}(\omega)]$ or, which is the same, $Z_0[T_{11}(\omega)-T_{22}(\omega)]+T_{12}(\omega)-Z_0^2T_{21}(\omega)=0$. But as $T_{11}(\omega)=T_{22}(\omega)$, this condition reduces to $T_{12}(\omega)-Z_0T_{21}(\omega)=0$. Calculations for orders 1–3 show again the existence of a family of frequencies $\tilde{\omega}_m=(3^n c/L)m\pi$.

As a conclusion, we have seen that, independent of the particular end conditions, some features of the eigenproblem remain invariant when shifting from one order to another. It would not then be surprising if other invariants were found, although it is not easy to predict them analytically.

Figure 3 shows the calculated eigenfrequencies for the first three orders with open ends (a), closed ends (b), and anechoic ends (c). This figure is useful to discover that a symmetry and a fractal organization of these frequencies appears in orders 2 and 3 (order 1 is actually just an expansion chamber made of three spans of equal length, so it cannot be considered a prefractal waveguide). For orders 4 and 5, the same kind of behavior can be seen if we go up to very high frequencies: as the order goes up, the eigenfrequencies tend to be independent of the end conditions. We can expect then that other features of the waveguide will also be independent of the end conditions for orders higher than 3.

The independency of the eigenfrequencies from the end conditions has also been verified experimentally with input impedance measurements obtained with the TMTC method [9] such as those presented in Fig. 4. The basic principle of this method is to use three pressure measurements on an acoustically cylindrical calibrated cavity placed at the input section of the waveguide to be explored. The pressure and acoustical velocity are derived at each frequency from these pressure measurements. To avoid any discontinuity problem, the diameter of the calibrated cavity has been chosen equal to that of the waveguide. All measurements are done in the time domain and the frequency responses are obtained through a Fourier transform done on a 1-s-length signal allowing 1-Hz accuracy in the frequency domain.

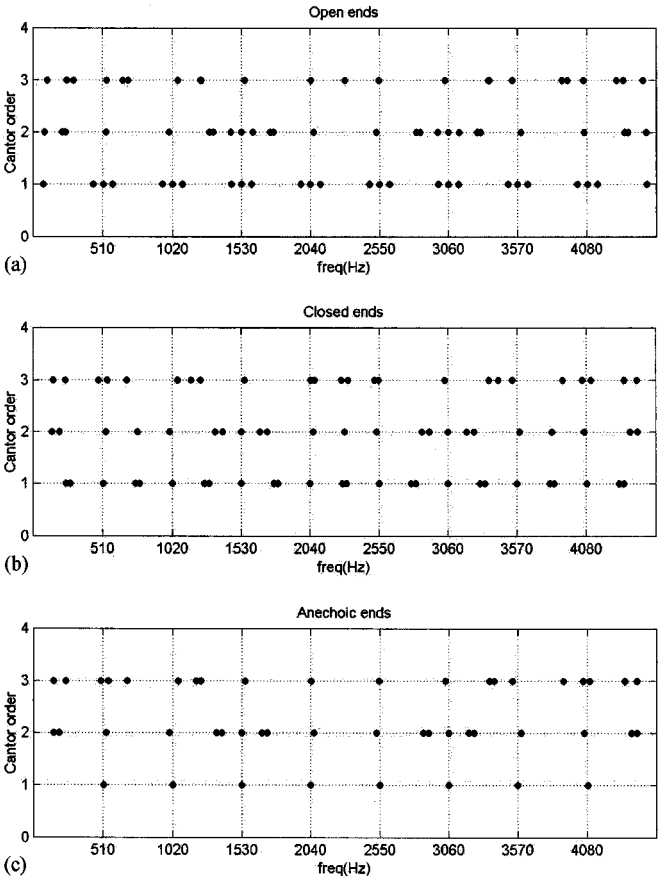

FIG. 3. Eigenfrequencies for Cantor waveguides of orders 1–3 with open (a), closed (b), and anechoic (c) end conditions.

The determination of the eigenfrequencies is just the first part of the whole eigenproblem. Their knowledge does not give any clue about the nature of the corresponding eigenmodes. In fact, for a general acoustical filter, they can be classed into two groups: extended modes and localized modes. The first are those that give important oscillations everywhere along the system (excepting of course the nodal points), whereas the second give noticeable vibrations in some zones but negligible ones in others or, which is the same, they are a superposition of propagating waves in some zones but evanescent waves in others. In the latter case, the eigenfrequencies are often called trapped frequencies.

Only a point-to-point exploration of the internal pressure distribution for each eigenfrequency can show if it corresponds to an extended wave or a localized one. This kind of computation is hard and time consuming in the frequency domain. This is the reason why a numerical time-domain calculation has been implemented. It is presented in the next section.

A rather different problem that can be explored through the transfer matrices is that of ''passing bands'' and ''nonpassing bands'' (sometimes called ''forbidden bands''). For a periodic repartition of the different diameter cylindrical spans, the calculation of Floquet's multipliers (which is the basis of Bloch's theory) is possible and gives direct information about the existence of passing and nonpassing frequency

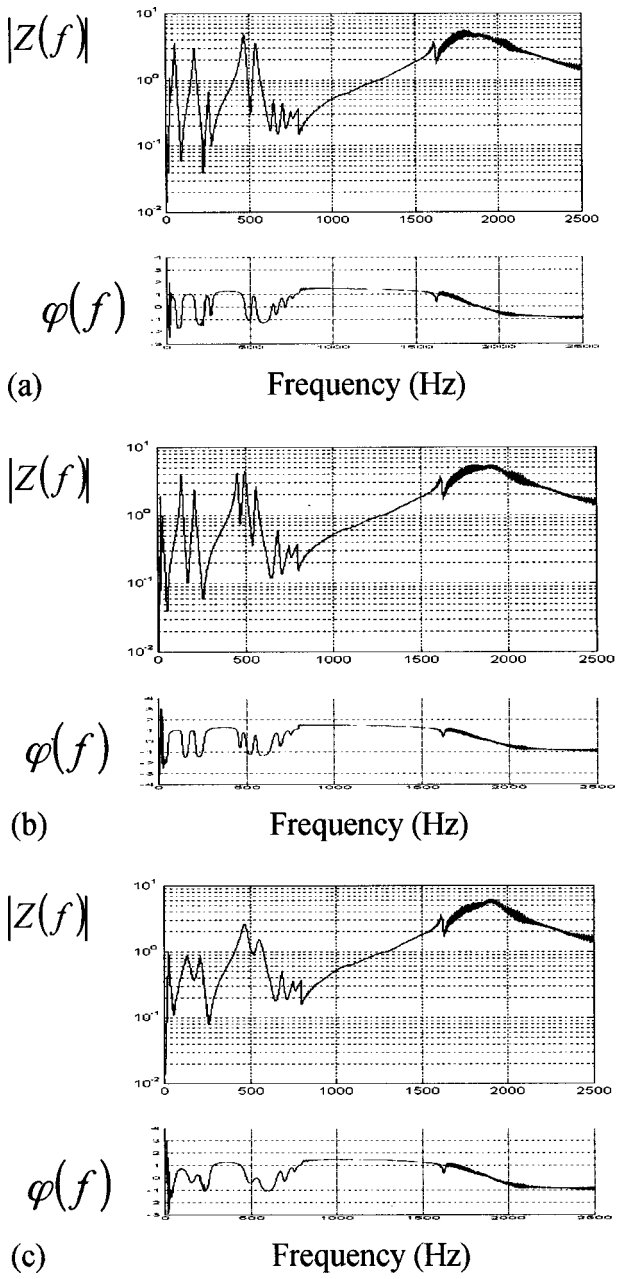

FIG. 4. Measured input impedances (amplitude, upper curves, and phase, lower curves) between 0 and 2500 Hz for a Cantor waveguide of order 3 with open (a), closed (b), and anechoic (c) output end conditions.

bands [10,11]. However this is not possible for a nonperiodic network.

The concept of ''forbidden frequencies'' deserves a comment. In general, a forbidden frequency is a frequency which, even if introduced at the filter input, does not reach the output section. As the acoustical impedance $\tilde{Z}(\omega)=\tilde{p}(\omega)/\tilde{v}(\omega)$ relates variables measured just at the input section, it does not give any information about forbidden and trapped frequencies. It is thus necessary to perform other kinds of calculations and measurements.

From a mathematical point of view, the existence of forbidden frequencies can be explored through the transmission loss coefficient $[T_L(\omega)]$, which is obtainable from the total transfer matrix. The general expression for $T_L(\omega)$ is

$$T_L(\omega)=10\ln\left(\frac{\tilde{p}_i}{\tilde{p}_o}\right)^2$$
$$=20\ln\left(\frac{1}{2}\left|T_{11}(\omega)+T_{22}(\omega)+Z_0T_{21}(\omega)+\frac{1}{Z_0}T_{12}(\omega)\right|\right),$$

where $\tilde{p}_i$ and $\tilde{p}_o$ are the incident and transmitted acoustical pressures, respectively. The incident pressure is not equal to the total pressure at the input section, it is just the outward propagating pressure. So from an experimental point of view the transmission loss $T_L(\omega)$ cannot be measured directly but is obtained from the input impedance and the difference pressure level $D_{PL}(\omega)=\tilde{p}_{output}(\omega)/\tilde{p}_{input}(\omega)$ between the input and output sections.

The analytical expression for the transmission loss coefficient is more complicated than the eigenfrequency equation, and it is difficult to conclude anything from it. The numerical calculation of this function and the corresponding graphical representation has been performed for orders 1 to 5, and the results are shown in Fig. 5. These graphics have two interesting characteristics. On one hand, they show homothetical behavior, that is, the transmission loss at any order looks very similar to that of the preceding/following order if a contraction/expansion by the factor 3 is done on the frequency axis (something that has actually been done in Fig. 5). On the other hand, the simple lobes appearing in $T_L(\omega)$ for order 1 split into several lobes for order 2, then each lobe splits again for the next order, and so on. This looks like fractal iterative process, and we will refer to it as ''geometrical fractality.'' Finally, it is worth pointing out that, as the order increases, passing bands and forbidden bands appear.

The depth and abruptness of the minima in $T_L(\omega)$ for any order are obviously overestimated. These peaks would be highly smoothed and partially attenuated if losses were taken into account. Experimental measurements of the output pressure have been done that confirm this point. However, as $T_L(\omega)$ cannot be measured directly (as mentioned before), the comparisons have been done on $D_{PL}(\omega)$. Figure 6 presents $D_{PL}(\omega)$ for a Cantor waveguide of order 3. Figure 6(a) shows the calculated $D_{PL}(\omega)$ without losses on a logarithmic scale. Its shape is very close to that of $T_L(\omega)$, though inverted. That means that any conclusion about the effect of losses on the $D_{PL}(\omega)$ minima can be applied to the peaks in $T_L(\omega)$. Figure 6(b) is again a calculated result but it includes losses. As usual, the high frequencies have been drastically attenuated. Finally, Fig. 6(c) shows the experimental result. Even if the comparison between these last two figures shows that the model for losses should be improved, the presence of a forbidden band between 800 Hz and 2500 Hz (the limit of our measurements) is obvious in both figures.

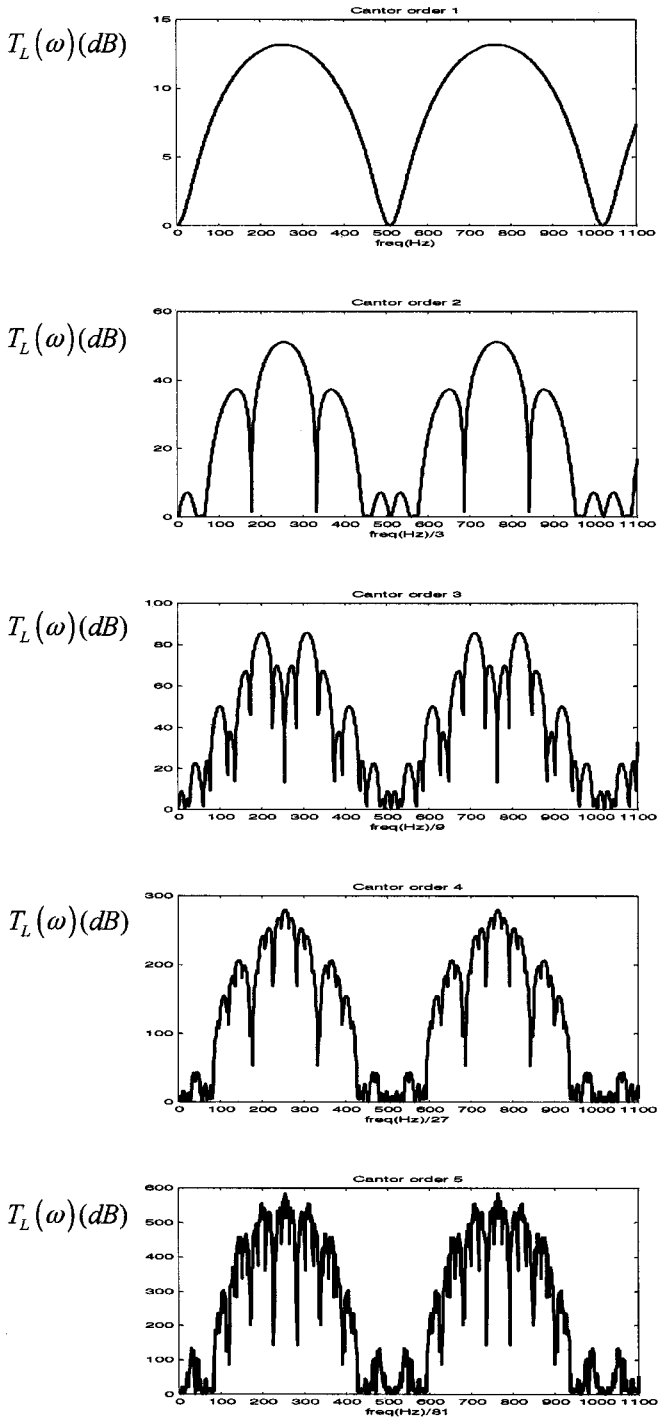

FIG. 5. Transmission losses of Cantor waveguides for orders 1–5.

C. Time-domain calculations

The time-domain numerical calculations correspond to a simulation of the reflection-transmission processes at the waveguide discontinuities: an impulse pressure wave $p_0\delta(t)$ has been propagated, transmitted, and reflected according to the local functions $r(t)$ and $t(t)$ mentioned in Sec. II. This calculation leads to a comb of various amplitude δ distributions, $\Sigma_i A_i \delta(t-t_i)$, which corresponds to the global pressure reflection function $R_p(t)$. The system frequency behavior can then be obtained through a Fourier transform. Since the measurements have been performed in a band limited frequency range, the numerical results have also been limited to the same band by numerical filtering. It is obvious from Fig. 7, presenting the superposition of the raw simulation result (without filtering), the simulation result filtered in the band 0–2500 Hz, and the measured reflection function for a Cantor waveguide of order 2, that the filtered simulation is in good agreement with the measured results.

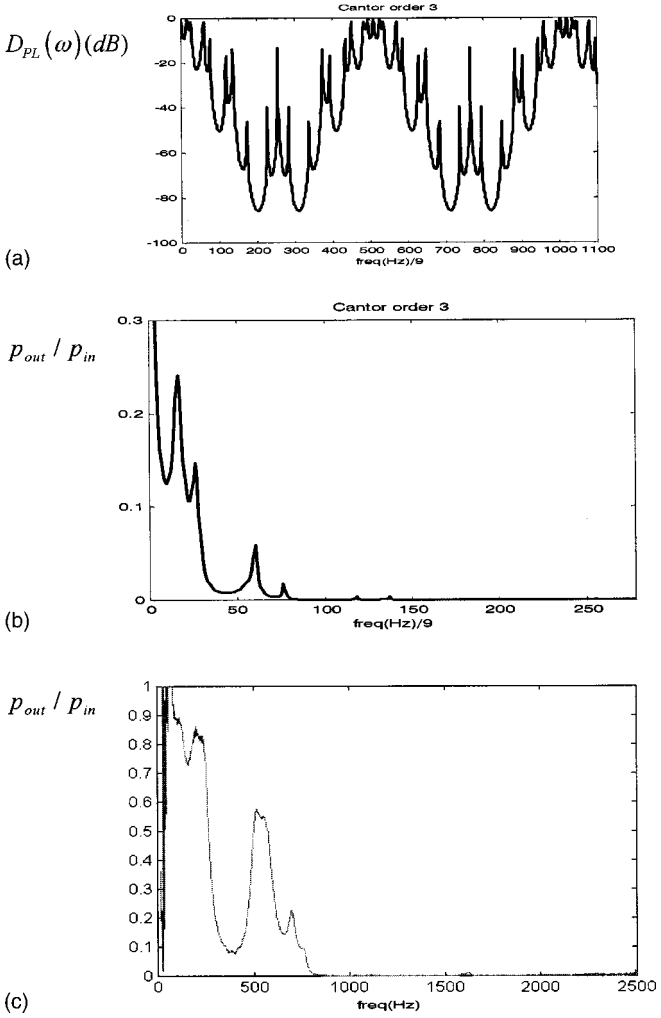

FIG. 6. Pressure ratio between the output and the input sections for a Cantor waveguide of order 3 with anechoic ends: numerical simulation without losses (a), numerical simulation with losses (b), and experimental measurement (c).

We have limited our simulations to order 5 because it is our highest physically feasible order. In this situation the length of the shortest uniform spans is 4 mm and is lower than their diameter. The basic hypothesis of plane wave propagation is no longer valid but it seems applicable since the numerical simulations (which do not take into account higher modes in the ducts) and the experimental results (which obviously include those higher modes) still show good agreement. The end conditions used were open $[r(t)=-\delta(t)]$, closed $[r(t)=\delta(t)]$, and anechoic $[r(t)=0]$. Those results are not shown here because at that

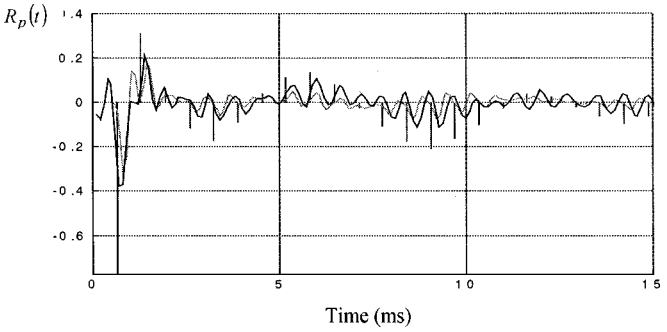

FIG. 7. Superposition of simulation results, without filtering (comb of delayed δ functions), filtered by a low pass numerical filter of cutoff frequency 2500 Hz (dotted line), and measured reflection function (continuous line) (with a bandwidth of 2500 Hz).

order of fractality they become very involved and difficult to read.

Figure 8 shows the computed time signal at the output end of Cantor orders 4 and 5. The most outstanding aspect is that the maximum intensity is not attained at the ballistic time but a few milliseconds later. It is worth pointing out that the signals obtained for these ''high'' orders present the typical features of a multidiffusion process as was said in Sec. II.

From these time-domain calculations it is possible to compute their frequency-domain equivalents, the global reflection coefficient $\tilde{R}(\omega)$ or the input impedance $\tilde{Z}(\omega)$. A comparison with experimental measurements is then possible. The plots of the input impedance (both calculated and experimental) for order 4 and various end conditions are shown in Fig. 9. The main discrepancies between the calculated and experimental curves appear for frequencies higher than 2000 Hz. They might be partly due to the absence of losses in the time-domain simulation and the existence of higher modes not taken into account. In any case, the comparison shows that the numerical model fits the experimental data sufficiently well. It is therefore assumed that the numerical results corresponding to the internal pressure field can be trusted.

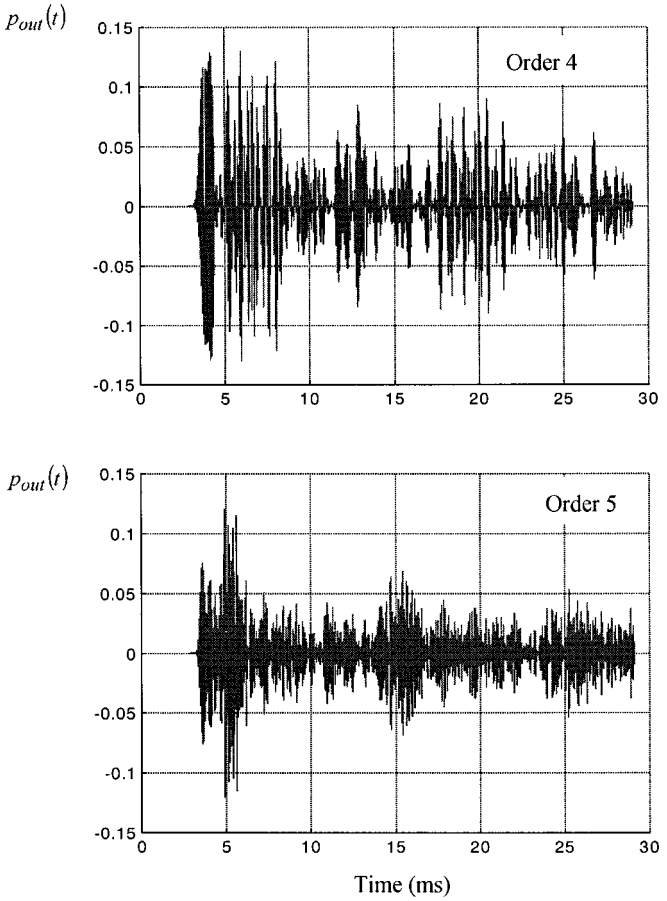

FIG. 8. Time-domain simulation of the output pressure for Cantor waveguide of orders 4 and 5 with open end conditions.

The same kinds of results have been obtained for a Cantor waveguide of order 5. The higher number of peaks and the fact that they are closer make the reading of the corresponding curves difficult (therefore they are not shown in this paper). The same features and conclusions mentioned in the previous paragraph appear.

IV. WAVE TRAPPING

As suggested in previous sections, an exploration of the internal pressure distribution along the Cantor waveguide has been performed in the time domain. The results have been Fourier transformed. An example of these results is presented for a Cantor waveguide of order 3 with closed ends on a logarithmic scale in Fig. 10. The input excitation is a $\delta(t)$ function which corresponds in the frequency domain to a flat spectrum.

It is difficult to extract precise information for the low frequency range (under 1000 Hz) because of the large width of the modes, but interesting features appear around 1500 Hz and 2300 Hz. At 1530 Hz a mode is clearly localized in the central span of the waveguide. This frequency corresponds roughly to a third resonance of the isolated central part (as the first resonance would be placed at 510 Hz, which corresponds to half a wavelength of 333 mm, the length of the central span). This frequency could also have been a resonance of the 111 mm parts if isolated with symmetrical end conditions; Fig. 10 shows that this is not the case when inserted in this Cantor waveguide. In any case, the wavelength corresponding to 1530 Hz would never fit the shortest spans (37 mm).

The nonresonance at 1530 Hz for the 111 mm parts can be understood by considering the symmetry of the waveguide. At a distance of half a wavelength, the central part (333 mm) has symmetrical end conditions. This is not the case for the 111 mm parts, which at the same distance present an expansion chamber at one side and a closed end at the other side.

The same kind of rationale can be applied to explain what happens around 2250 Hz where there is another localized wave, corresponding roughly to a fourth resonance of the isolated central span. However, the immediately higher resonance (at about 2300 Hz) seems to be an extended one.

The existence of localized modes is also possible in principle in the low frequency range, but there are so many close resonances in this zone that we do not dare to conclude anything definite. In any case, there is some suspicion of local-

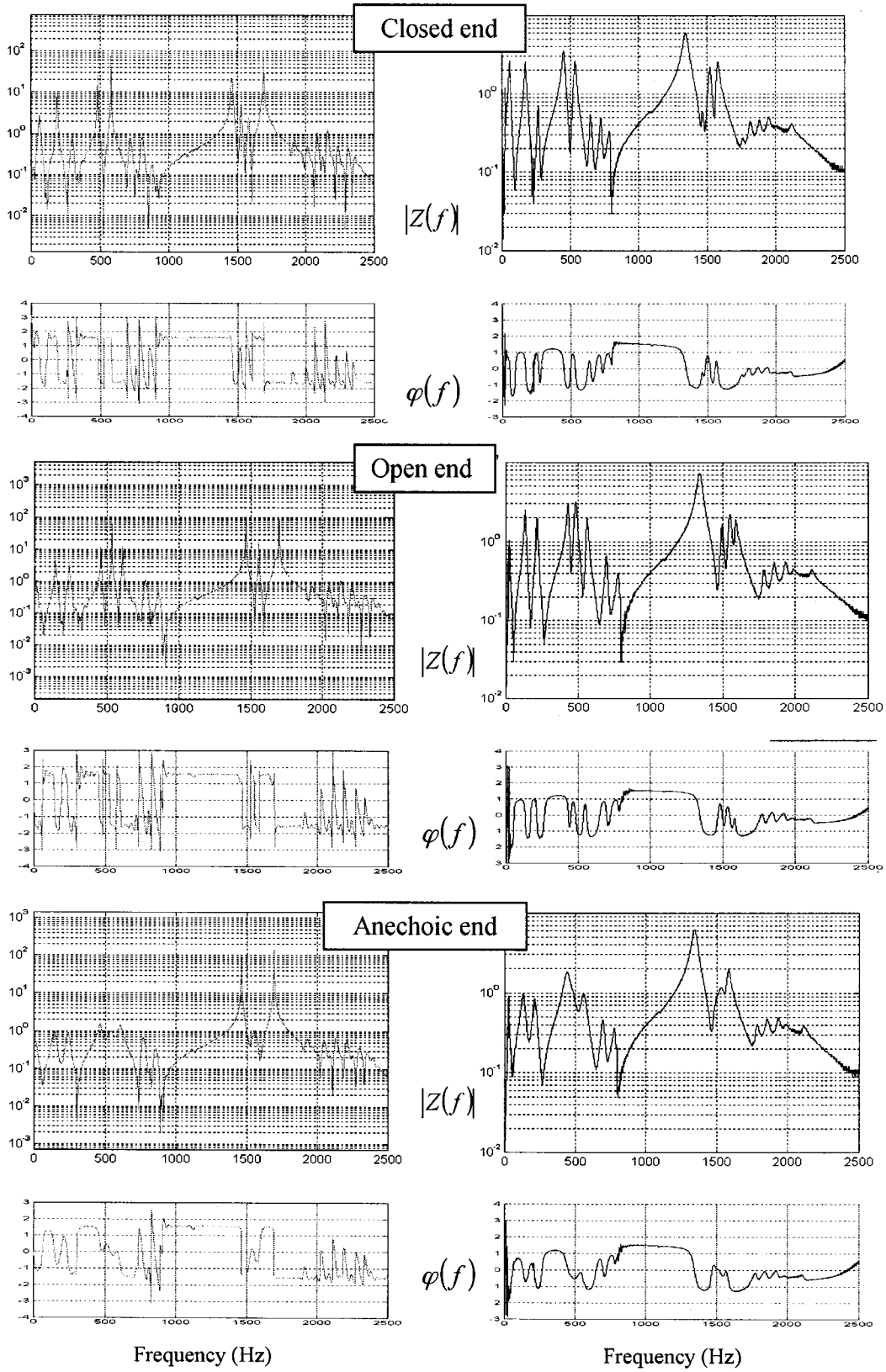

FIG. 9. Input impedance measured and computed between 0 and 2500 Hz from time-domain simulation for a Cantor waveguide of order 4 with open, closed, and anechoic conditions (amplitude, upper curves, and phase, lower curves).

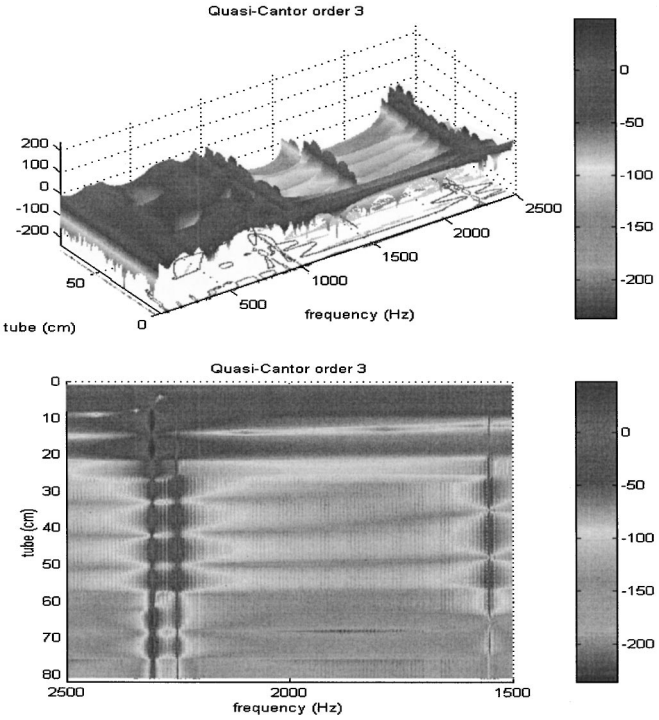

FIG. 10. Simulated internal pressure distribution for a Cantor waveguide of order 3 with closed ends.

ized modes around 500 Hz and 1000 Hz.

The study of other end conditions (open or anechoic) has proved that the existence of these spatially confined frequencies is independent of the particular end conditions.

As pointed out before, the experimental verification of localized modes is difficult, as any internal measurement drastically perturbs the wave propagation. We did carry out some point measurements to check the high amplitude decay of the acoustical pressure in the side spans: for frequencies of 530 Hz and 1020 Hz the modes seem to be localized in the central part. This has been verified experimentally with pressure measurements done on two points of the central span.

V. CONCLUSION

A prefractal acoustical system based on the geometry of the Cantor set has been built and studied from both a theoretical and an experimental (measurements and numerical simulations) point of view. Our results confirm in a totally different acoustical system those obtained by Alippi *et al.* [2]. Trapped or localized modes have been shown in the central part of the system for waveguides of order higher than 2.

The behavior of the Cantor waveguide in the frequency and time domains has proved to be rather independent of the boundary conditions for orders higher than 2.

It has been shown that the fractality of the physical system appears in its frequency responses. The mean shape of a frequency response at order $n+1$ can be obtained from that at order n through an expansion of the frequency axis by a factor of 3. This homothetical process is valid for n greater than 3. This provides the possibility of an expansion of both passing bands and forbidden bands. A question that has not been studied in this paper is whether this particular behavior comes from the fractality (or more precisely the homothetical character of the waveguide) or just from the existence of different length scales in the waveguide. The second hypothesis seems to be confirmed by some experiments (measurements and numerical simulations) made with the same elements used to build the Cantor waveguide but distributed randomly.

ACKNOWLEDGMENTS

The authors would like to thank the French Ministry of Foreign Affairs and the Spanish Ministry of Education and Culture for funding this work through a France-Spain Integrate Action. The authors want to acknowledge Yek Tran Ke and Doriane Mariani for their collaboration in the experimental measurements and Professor Werner Lauterborn for fruitful discussions.

[1] S. Alexander and R. Orbach, J. Phys. (France) Lett. **43**, L625 (1982).

[2] A. Alippi, A. Bettucci, F. Craciun, E. Molinari, and A. Petri, in *Proceedings of the IEEE Ultrasonics Symposium*, edited by M. Levy and B. R. McAvoy (IEEE, New York, 1991), pp. 399–402.

[3] E. Troncet, G. Ablart, and L. Allam, IEEE Trans. Antennas Propag. **46**, 434 (1998).

[4] A. Petri, A. Alippi, A. Bettucci, F. Craciun, F. Farrelly, and E. Molinari, Phys. Rev. B **49**, 15 067 (1994).

[5] B. Sapoval and Th. Gobron, Phys. Rev. E **47**, 3013 (1995).

[6] B. Sapoval, O. Haeberlé, and S. Russ, J. Acoust. Soc. Am. **102**, 2014 (1997).

[7] P. M. Morse, *Vibration and Sound*, 2nd ed. (McGraw-Hill, New York, 1948), Chap. III, Sec. 12, pp. 122–125.

[8] F. Fahy, *Foundations of Engineering Acoustics* (Academic, San Diego, 2001), Chap. 8, Sec. 863, p. 205. Other examples can be found in numerous books.

[9] V. Gibiat and F. Laloë, J. Acoust. Soc. Am. **88**, 2533 (1990).

[10] F. Bloch, Z. Phys. **52**, 555 (1928).

[11] O. Richoux, Ph.D. thesis, Université du Maine, Le Mans, France, 1999.